

ANALYTICAL SOLUTION FOR CALCULATION OF BEARING CAPACITY OF SHALLOW FOUNDATIONS ON GEOGRID-REINFORCED SAND SLOPE*

V. ROSTAMI^{1**} AND M. GHAZAVI²

¹Faculty of Engineering, Science and Research Branch, Islamic Azad University, Tehran, I. R. of Iran
Email: Rostami@iauh.ac.ir

²Dept. of Civil Engineering, K. N. Toosi University of Technology, Tehran, I. R. of Iran

Abstract– The bearing capacity of foundations resting on slopes is commonly calculated using empirical equations. In recent years, it has been demonstrated that geosynthetic reinforced soil can enhance the foundation bearing capacity. In this paper, an analytical method for determination of the ultimate bearing capacity of surface strip footing on a sand slope reinforced with geogrid layers is presented. The angle of the slope with the horizontal direction is varied within 20° to 40°. In this study, the Coulomb-type lateral earth pressure theory has been used to compute the foundation bearing capacity. It is assumed that geogrid layers act such that the active earth pressures are reduced. The results obtained from the proposed method are compared with experimental and numerical results. Parametric studies have also been performed to show the effects of contributing parameters such as number of geogrid layers, locations of reinforcement layers, soil properties and the slope angle on the bearing capacity of strip foundations resting on the reinforced sand. The results indicate that the magnitude of bearing capacity of strip footings on the sand slope can be significantly increased by using geogrid layers.

Keywords– Geogrid-reinforced slope, strip footing, bearing capacity, shallow foundation

1. INTRODUCTION

Sometimes foundations are built on slope or near the slope crest such as roads or buildings constructed in hilly regions and foundations for bridge abutments resting on granular fill slopes. The bearing capacity of footing rests on slopes depends on the stability of slope and the soil bearing capacity. The construction of a footing on sloping ground usually results in the footing bearing capacity reduction as compared to that constructed on horizontal ground surface, depending on the geometry of the footing and slope geometry as well as the location of the footing with respect to the slope crest. The bearing capacity of footings on loose soil may be improved by using reinforcement objects such as anchors, stone columns, steel bars, and geosynthetics. In general, the use of geosynthetics to increase the bearing capacity and decrease the settlement of shallow foundations has been shown to be efficient [1]. In recent years, many experimental and analytical solutions have been presented for achievement acceptable footing bearing capacity by locating footings on reinforced soils. In this situation, the use of reinforcement layers may be useful to compensate the footing bearing capacity reduction.

Few studies on the bearing capacity behavior footings resting on reinforced soil slopes have been reported in the literature. Khing et. al. [2] conducted laboratory-model tests to evaluate the bearing capacity of a strip foundation supported on a sand layer reinforced with geogrid layers. They showed that, the bearing-capacity ratio at limited levels of settlement is about 67- 70% of the bearing-capacity ratio calculated on the basis of the ultimate bearing capacity. Omar et al. [3] conducted laboratory model test investigating of the ultimate bearing capacity of strip and square foundations supported by geogrid

*Received by the editors February 13, 2013; Accepted May 17, 2014.

**Corresponding author

reinforced sand. They evaluated the critical depth of reinforcement and the dimensions of geogrid layers to achieve the maximum bearing-capacity. Shin et al. [4] conducted small-scale laboratory model tests for foundations rest on geogrid-reinforced clayey soils. They showed that, in general, the ultimate and allowable bearing capacities of foundations can be improved by incorporating geogrid reinforcement. Yoo [5] conducted laboratory model tests and finite element model to determine the bearing capacity of a strip footing on a geogrid-reinforced earth slope. They evaluated the effects of geogrid length, number of geogrid layers, vertical spacing and depth to topmost layer of geogrid on the footing bearing capacity. Their results indicate that the bearing capacity of strip footings on sloping ground can be increased by using geogrid layers. This increase depends mostly on the number of geogrid layers and their locations. Vafaeian and Abbaszadeh [6] studied the behavior of steep reinforced slopes under the effect of external loading on the surface. They used small-scale model tests and showed that with increasing the spacing between reinforcement layers, the failure external load decreased. El Sawwaf [7] evaluated the behavior of strip footing on geogrid reinforced sand over a soft clay slope. For this purpose, a model footing with 75 mm width and geogrids was used. Test results showed that the inclusion of geogrid layers in the replaced sand improves the footing load-settlement performance. They found that with increasing the number and lengths of geogrid layers significant improvement in the footing bearing capacity was achieved. Alamshahi and Hataf [8] performed a series of numerical and model tests on geogrid reinforcement and grid-anchor layers to evaluate the bearing capacity of a strip footing resting on reinforced sand slopes. The results showed that load-settlement behavior and bearing capacity of the rigid footing can be considerably improved by using a reinforcing layer at the appropriate location in the slope. Sommers and Viswanadham [9] performed laboratory tests to evaluate the behavior of strip footing on geotextile-reinforced slopes. They used small-scale physical tests in large beam centrifuge to simulate field prototype conditions and examined the stability of geotextile-reinforced slopes subjected to a vertical load applied to a strip footing. Their results showed that the vertical spacing between reinforcement layers has a significant impact on the stability of reinforced slope, and distributions of peak strains in reinforcement layers due to the strip footing placed on the surface of the reinforced slope were found to extend up to mid-height of the slope and thereafter they were found to be negligible. Choudhary et al. [10] investigated the bearing capacity behavior of strip footing on reinforced fly ash slope. They conducted laboratory model tests covering a wide range of boundary conditions. The results showed that the pressure settlement behavior and the ultimate bearing capacity of footing resting on the top of a fly ash slope can be affected by the presence of reinforcing layers. During the last three decades, a large number of small-scale laboratory model tests and large scale tests conducted to evaluate the ultimate and allowable bearing capacities of shallow foundations supported on sand reinforced with geogrid layers [11-23]. Despite significant attempts to date devoted to enhancing the footing load-carrying characteristics, it is still essential to develop solutions for computing the ultimate bearing capacity of strip footings on reinforced slopes. To this aim, fundamental mechanisms governing the load carrying capacity of shallow foundations on reinforced soil must be investigated. This is essential for practicing engineers in the design and construction of footings. For this purpose, this paper presents a closed form solution for determination of the bearing capacity of strip foundations constructed on geosynthetics reinforced soil using a limit equilibrium approach based on the Coulomb type lateral earth pressures exerted on a rigid retaining wall. Parametric studies are also carried out to determine the effects of soil reinforcement, soil parameters, and slope geometries on the surface footing bearing capacity.

2. ANALYSIS OF BEARING CAPACITY

The footing bearing capacity factors may be determined as suggested by Terzaghi [24] in terms of soil parameters such as internal friction angle of soil and soil cohesion. Equation (1) shows Terzaghi bearing capacity formula for strip footing.

$$q_u = cN_c + qN_q + 0.5 B \gamma N_\gamma \quad (1)$$

where N_c , N_q , and N_γ are the bearing capacity factors, c is soil cohesion, q is surcharge, γ is soil unit weight, and B is the foundation width. Richards et al. [25] made a simplification to the Prandtl failure surface as shown in Fig. 1. This assumption leads to estimating the fan-shaped transition zone and thereby averaging its effect concentrating on the shear transfer at line AC, which can then be thought of as an imaginary retaining wall with the active lateral thrust P_A from region ABC, pushing against the passive resistance P_P from region ACD (Fig. 1). Using the force equilibrium in the horizontal direction on imaginary wall AC (Fig. 1), the bearing capacity factors may be determined as [25]:

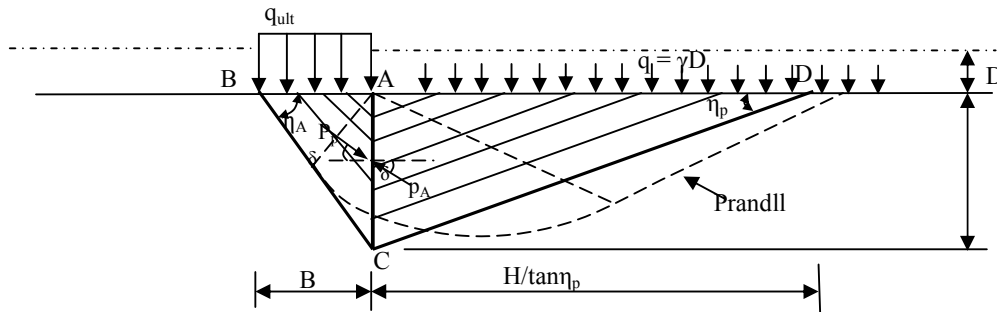


Fig. 1. Simplification to the Prandtl failure surface by Richards et al. [23]

$$N_q = K_p / K_A \quad (2)$$

$$N_\gamma = \tan \eta_A \left(\frac{K_p}{K_A} - 1 \right) \quad (3)$$

where η_A is angle between line AB with the horizontal direction (Fig. 2), and K_A and K_p are the active and passive lateral earth pressure coefficients, respectively and are given by:

$$K_A = \frac{\cos^2 \varphi}{\cos \delta \left\{ 1 + \sqrt{\frac{\sin(\varphi + \delta) \sin \varphi}{\cos \delta}} \right\}^2} \quad (4)$$

and

$$K_p = \frac{\cos^2 \varphi}{\cos \delta \left\{ 1 - \sqrt{\frac{\sin(\varphi + \delta) \sin \varphi}{\cos \delta}} \right\}^2} \quad (5)$$

The angles of active and passive wedges with the horizontal direction respectively are:

$$\eta_A = \varphi + \tan^{-1} \left\{ \frac{[\tan \varphi (\tan \varphi + \cot \varphi) (1 + \tan \delta \cot \varphi)]^{1/2} - \tan \varphi}{1 + \tan \delta (\tan \varphi + \cot \varphi)} \right\} \quad (6)$$

$$\eta_p = -\varphi + \tan^{-1} \left\{ \frac{[\tan \varphi (\tan \varphi + \cot \varphi) (1 + \tan \delta \cot \varphi)]^{1/2} + \tan \varphi}{1 + \tan \delta (\tan \varphi + \cot \varphi)} \right\} \quad (7)$$

In this paper, the above simple mechanism is used to compute the bearing capacity of strip foundations on geogrid reinforced soil slope.

3. BEARING CAPACITY OF REINFORCED SOIL SLOPE

In reinforced soil, active and passive wedges in terms of Coulomb mechanism and equilibrium equations in the horizontal and vertical directions can be written to calculate the bearing capacity. Figure 2 shows a

given reinforcement layer located at u from the foundation bottom. This layer tolerates tensile force and thus the active force is reduced. For simplicity, it is assumed that the foundation is located at the ground surface with no embedded depth (Fig. 2). The pull out force in geogrid (Fig. 4) is computed from:

$$F_R = 2L\sigma_v \tan \phi_u \tag{8}$$

where L is the length of geogrid that provides frictional force between soil and geogrid along it, σ_v is vertical stress at depth z , ϕ_u is soil-geogrid interface friction angle, and F_R is the resultant of longitudinal shear stresses acting on both sides of reinforcement per unit width (Fig. 3). The tensile force on the reinforcement layer is determined from:

$$T = F_R \cdot w \tag{9}$$

where w is width of reinforcement materials. In Fig. 4, assuming $L = m \cdot B$, $u = n \cdot B$, and $w = 1$, the total pull out force on geogrid layer is calculated using:

$$T = 2(\gamma u + q) \tan \phi_u L \tag{10}$$

From Fig. 3, H is given by:

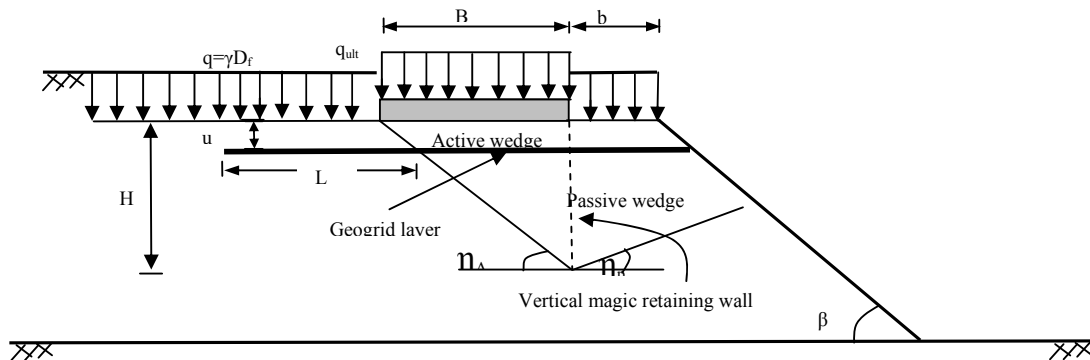


Fig. 2. Proposed failure mechanism for reinforced soil-footing system

$$H = B \tan \eta_A \tag{11}$$

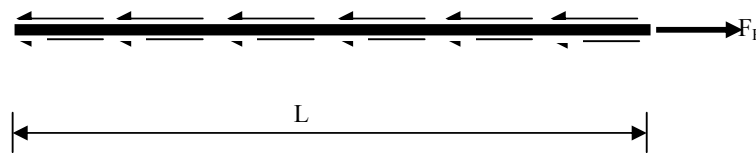


Fig. 3. Pull out force acting on each geosynthetic layer

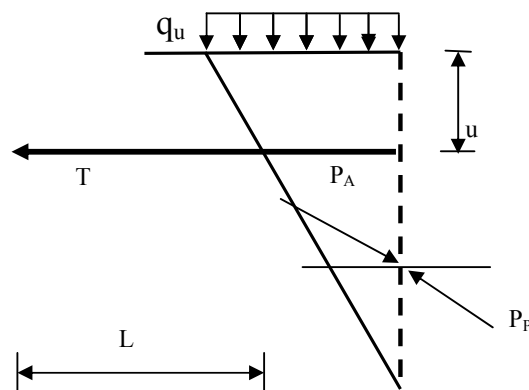


Fig. 4. Active wedge and reinforcement layer

Having all parameters, the equilibrium equation can be written for all forces acting on the active and passive wedges (Fig. 5). The above procedure can be applied to a foundation on soil reinforced with more than one geogrid layer. Figure 5 shows N geogrid layers each of which has length $L=m.B$. The top layer of reinforcement is located at depth u_1 from the footing bottom. The second layer is located at u_2 from the first layer. In this manner, other geogrid layers are located at u_3, u_4, \dots, u_N . The lowest geogrid layer is located at H below the foundation where:

$$u_1 + u_2 + u_3 + \dots + u_N = H \tag{12}$$

Assuming: $u_1 = u_2 = u_3 = \dots = u_N$ the pull out force for each reinforcement layer is:

$$T_1 = 2(q + \gamma u_1) \tan \varphi_u L \tag{13a}$$

$$T_2 = 2(\gamma(u_1 + u_2) + q) \tan \varphi_u L \tag{13b}$$

$$T_3 = 2(\gamma(u_1 + u_2 + u_3) + q) \tan \varphi_u L \tag{13c}$$

$$T_N = 2(\gamma(u_1 + u_2 + u_3 + \dots + u_N) + q) \tan \varphi_u L \tag{13d}$$

The pull out forces for each reinforcement layer is (Fig. 5):

$$T_N = 2(N \gamma u_1 + q) \tan \varphi_u L \tag{14}$$

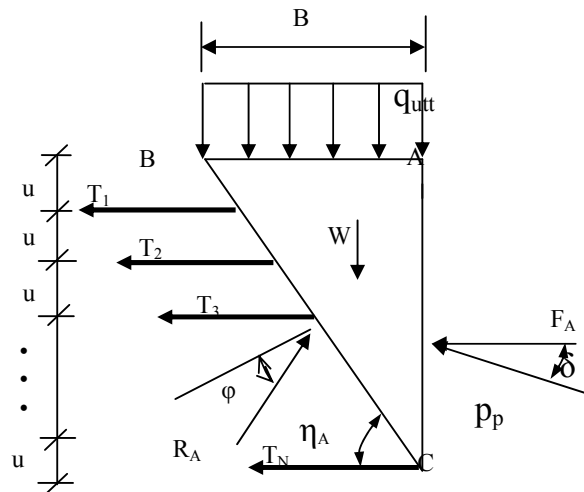


Fig. 5. Contributing forces acting on active wedge

Taking equilibrium equation in X direction, R is computed from:

$$\sum F_x = 0 \Rightarrow R_A \cos(90 - \eta_A + \varphi) - \sum_{i=1}^N T_i - P_p \cos \delta = 0 \tag{15}$$

The ultimate bearing capacity can be calculated using:

$$q_{ult} = \frac{-W + P_p \sin \delta + (\sum_{i=1}^N T_i + P_p \cos \delta) \cot(\eta_A - \varphi)}{B} \tag{16}$$

Assuming $b=0$, the values of K_p and η_A are calculated from:

$$K_p = \frac{\cos^2 \varphi}{\cos(-\delta) \left\{ 1 - \sqrt{\frac{\sin(\varphi + \delta) \sin(\varphi + \beta)}{\cos(-\delta) \cos(-\beta)}} \right\}^2} \quad (17)$$

$$\eta_A = \varphi + \tan^{-1} \left\{ \frac{[\tan(\varphi - \beta)(\tan(\varphi - \beta) + \cot \varphi)(1 + \tan \delta \cot \varphi)]^{1/2} - \tan(\varphi - \beta)}{1 + \tan \delta (\tan(\varphi - \beta) + \cot \varphi)} \right\} \quad (18)$$

Substituting all pull out forces from Eq. (14) and assuming $D_i=SB$ and $b=0$ gives the ultimate bearing capacity as:

$$q_{ult} = \frac{1}{2} \gamma B \left[\left[K_p \tan^2 \eta_A (\sin \delta + \cos \delta \cot(\eta_A - \varphi)) - \tan \eta_A \right] + 4(S + mn \sum_{i=1}^N N_{i=1}) \tan \varphi_u \cot(\eta_A - \varphi) \right] \quad (19)$$

The bearing capacity factor for layered reinforcement condition is given by:

$$N_\gamma = \left[\left[K_p \tan^2 \eta_A (\sin \delta + \cos \delta \cot(\eta_A - \varphi)) - \tan \eta_A \right] + 4(S + mn \sum_{i=1}^N N_{i=1}) \tan \varphi_u \cot(\eta_A - \varphi) \right] \quad (20)$$

4. VERIFICATION

In this section, the results obtained from the present analytical solution using limit equilibrium method are compared with the results obtained from a number of results reported by others.

a) Comparison with experimental results

Yoo [5] performed laboratory model tests to study the bearing capacity behavior of a strip footing on a geogrid-reinforced slope. A steel test box with inside dimensions of 1.8×0.5 m in plan and 1.2 m in height was used. The box was sufficiently rigid to maintain plane strain conditions in the reinforced slope models. In all tests, an artificial slope of 1H:0.67V was used and the model footing was loaded using a hydraulic jack at a speed of 1.0 mm/min. He used sand by a raining technique with a specially designed hopper system. The effective size (D_{10}), uniformity coefficient (C_U), and coefficient of curvature (C_c) for the sand were 0.36, 1.61, and 1.1 mm, respectively, the estimated internal friction angle at the relative density of 70% was approximately 42°. Biaxial geogrids were used that have tensile strength 55 kN/m at a maximum strain of 12.5%. The nominal thickness and the aperture size are 1.0 mm and 20×20 mm, respectively. The experimental results found by Yoo [5] are compared with the present analytical study in Fig. 6. The increase in the ultimate bearing capacity due to the inclusion of reinforcement has been expressed in the form of a non-dimensional term named the bearing capacity ratio, $BCR=q_{uR}/q_u$, where q_{uR} is ultimate bearing capacity of footing on reinforced soil and q_u is ultimate bearing capacity of the same footing on unreinforced soil. It is noted that the footing ultimate bearing capacity was determined as the pressure corresponding to a footing settlement of 10%B. As seen, there is very good agreement between experimental and analytical results. Figure 6 shows that when the one geogrid layer is used the difference between analytical and experimental results is about 31%. For 2 and geogrid layers, these differences account for about 5.4% and 0.6%, respectively. In general, there is a satisfactory agreement between these data, especially for more geogrid layers.

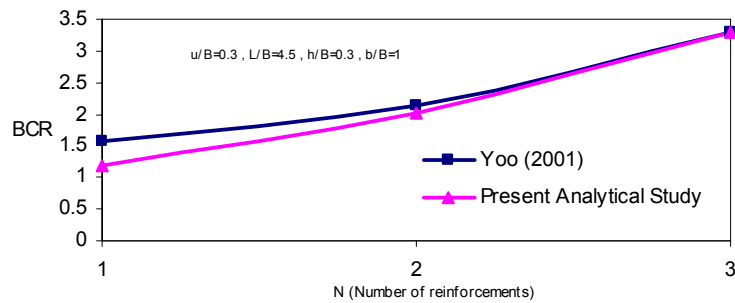


Fig. 6. Comparison of present analytical results with experimental tests by Yoo [5]

b) Comparison with numerical results

In this section, the results obtained from the present analytical approach are compared with numerical results reported by Thanapalasingam and Gnanendran [26] who performed 3D numerical analyses based on FLAC3D on footing characteristics near a slope. They used strain softening failure criterion with non-linear stiffness behavior using Duncan's method. Geogrid SELs element given in FLAC3D program was also used to model the structural behavior of geogrid layer on the interaction of soil-geogrid. They used only 2 reinforcement layers at 0.25B, 0.5B, 0.75B, 1.0B, 1.25B, 1.5B from the footing bottom.

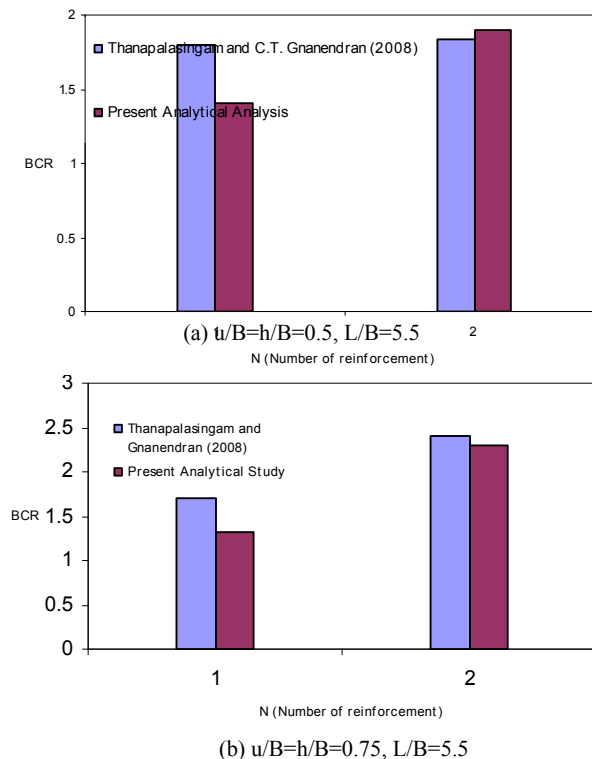


Fig. 7. Comparison between present analytical results with numerical results reported by Thanapalasingam and Gnanendran [24]

The sandy soil had a Poisson's ratio of 0.3 and an internal friction angle of 42° . Other properties were coupling spring stiffness per unit area= 1×10^{10} N/m³, elastic modulus area= 1×10^{10} N/m³, and bulk modulus exponent=0.50, the slope angle was 2H:1V. The values of BCR predicted by the present analytical solution with those predicted from numerical analyses are compared.

In Fig. 7, as observed, when $N=1$ geogrid layer is used, the difference between the two methods is about 29%. For $N=2$, this difference accounts for about 4.3%. There is generally good agreement between analytical and numerical data.

c) Comparison with experimental results

Alamshahi and Hataf [8] performed a series of model tests on geogrid and grid-anchor layers to evaluate the bearing capacity of a strip footing resting on reinforced sand slopes. For this purpose, they performed a series of laboratory model tests in a steel test box having inside dimensions of 1.3×0.5 m and 0.6 m height. The slope was 1H:0.67V, which makes an angle of 33.8° in the horizontal direction. The model steel strip footing was 499 mm long, 100 mm wide, and 10 mm thick. The footing was located on the crest of the slope at $0.5B$ from the slope edge. For soil reinforcement, geogrid and grid-anchor made of high-density polyethylene was used. The geogrid sheets had mesh aperture 27×27 mm and a maximum tensile strength of 5.80 kN/m. Gridanchor also had a mesh aperture 8×6 mm and a maximum tensile strength of 5.8 kN/m. The sand used was medium to coarse, washed, and dried, and had rounded to sub-rounded particles. The maximum and the minimum dry unit weights of the sand were found to be 19 and 13.4 kN/m^3 . The uniformity coefficient (C_u) and coefficient of curvature (C_c) for the sand were 7.78 and 1.24, respectively. The sand internal friction angle at 70% relative density was approximately 38° . They defined the BCR value as the footing pressure on the reinforced slope ($q_{\text{reinforced}}$) to that of the same footing on the same slope with no reinforcement (q). They considered these pressures corresponding to a settlement equal to $5\%B$ as the footing bearing capacity. As also stated, the bearing capacity for the model footing was determined from the load-settlement variation such that after these pressures the footing was assumed to collapse. Figure 8 shows results obtained from the present analytical method and experimental result performed by Alamshahi and Hataf [8]. As seen, when one reinforcement layer is used, the difference between the footing bearing capacity predicted by the present method and that reported from experimental results is 2.56%. For 2 layers, this difference accounts for about 2.8%.

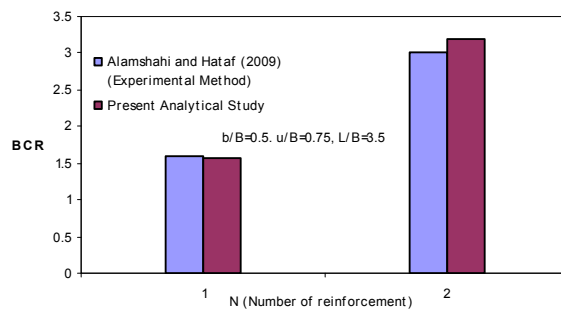


Fig. 8. Comparison between present analytical results with experimental results reported by Alamshahi and Hataf [8]

5. PARAMETRIC STUDIES

a) Effect of footing distance from slope crest

Based on the present analytical method, the effect of the distance of the footing from the slope crest is investigated as shown in Fig. 9. It is obvious that when this distance increases, the passive wedge is enlarged, resulting in increasing the footing bearing capacity. To evaluate the bearing capacity of a footing close to the slope crest, a simplification may be made as shown in Fig. 9. For this purpose, passive ABCM wedge may be replaced with AB'M. For this wedge, it is assumed that AC' extends from the footing edge

to the slope toe and makes angle β_1 . In fact, in this simplification, the effect of wedge ABCM is similar to wedge AB'M, noting that both wedges have the same area and thus the same weight. Angle β_1 can be computed from:

$$\beta_1 = \tan^{-1} \left[\frac{(\tan \eta_a - s \tan \eta_p)^2 \cdot \sin \beta \cdot \sin \eta_p}{\tan^2 \eta_a \cdot \sin(\eta_p + \beta) - (\tan \eta_a - s \tan \eta_p)^2 \cdot \sin \beta \cdot \cos \eta_p} \right] \quad (21)$$

where η_a and η_p are the angles of active and passive wedges with the horizontal direction respectively and $s=b/B$ is the distance ratio.

To compute q_{ult} for the footing shown in Fig. 9, Eq. (20) may be used with β_1 instead of β . Figure 10 shows the variation of β_1 versus $s=b/B$. As seen, by increasing s , the value of β_1 decreases, the s value decreases and thus the footing bearing capacity decreases. As seen in Fig. 10, for a slope angle of $\beta=30^\circ$, when $\phi=30^\circ$, by increasing the distance ratio up to 3, β_1 decreases to almost zero and this means that the effect of slope angle has very negligible effect on the footing bearing capacity. For $\phi=40^\circ$, increasing the distance ratio up to 5, β_1 decreases to almost zero. This also means that the edge distance affects the footing bearing capacity when it is smaller than five times the footing width. The above finding was supported by others.

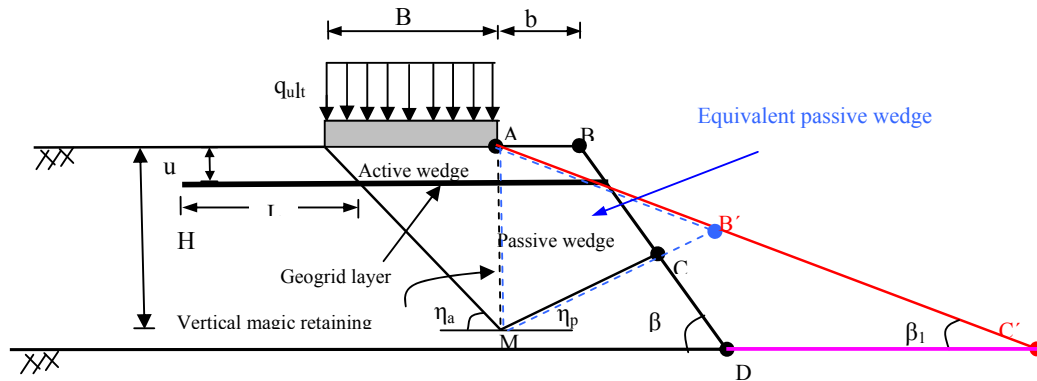


Fig. 9. Passive wedge simplification

For example, Meyerhof [27] reported that the footing bearing capacity factors for a strip foundation in purely cohesive and cohesionless materials decrease with greater inclination of the slope and increase rapidly with greater foundation distance from the edge of the slope. Beyond a distance of about 2 to 6 times the foundation width (depending on ϕ and footing embedment), the bearing capacity is independent of the inclination of the slope and becomes the same as that of a foundation on the horizontal ground surface.

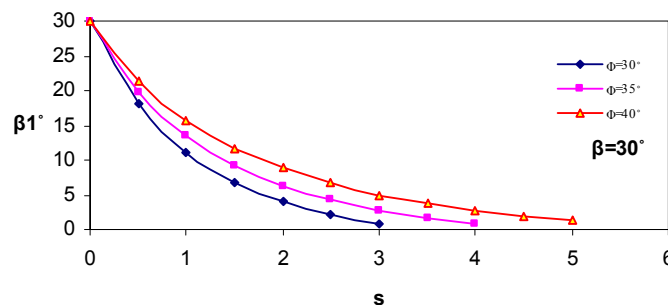


Fig. 10. Variation of β_1 versus s

Lee and Manjunath [28] also performed a series of tests to evaluate of effect of edge distance of the footing from the slope crest. For this purpose, five different distances for the footing on both reinforced and unreinforced soil with 2H:1V slope were used. These distances were $b=1B, 2B, 3B, 4B$ and $5B$. $u=0.5B$ was used for reinforcement embedment depth. Their results indicate that for both reinforced and unreinforced slopes, the ultimate bearing capacity increased with increasing the edge distance. They showed that at edge distance of $5B$, the ultimate bearing capacity of the footing on the slope approached that of a footing on a flat surface for both reinforced and unreinforced soil. They also found that the effect of the slope was minimized when the footing was placed at an edge distance beyond $5B$. In addition, it was shown that for other smaller edge distances, the footing bearing capacity on the reinforced slope was considerably greater than that of the footing on unreinforced slope. Choudhary et al. [10] conducted tests on strip footing resting on flyash slope at varying edge distances from the slope crest. These distances were $b=1B, 2B$, and $3B$ for both unreinforced and reinforced soil. They showed that the footing ultimate bearing capacity for a given slope remained almost constant and identical to that of the footing on the horizontal surface when the edge distance increased beyond $3B$. El Sawwaf [7] conducted tests and reported that if the footing was placed at a distance of $2B$ or further from the slope crest, the bearing capacity improvement (BCR) becomes insignificant. Also, it showed that the BCR value decreased with increasing b from $1.5B$ to $3B$ [5]. Based on the current research, the maximum value of b to have the complete passive wedge is equal to $(\tan\eta_a/\tan\eta_p)$. Thus, the footing distance from the slope crest depends on soil properties, slope geometry, and footing width. When the friction angle of cohesionless material, ϕ , varies in the practical range of $30-40^\circ$, the edge distance to form complete passive edge from the slope crest varies in $3.1B$ to $5.4B$ range. This range is in good agreement with above findings reported by others. Table 1 shows b/B ratio range reported, obtained from experimental and analytical studies performed on reinforced and unreinforced soil slope. As seen, there is very good agreement between the present analytical prediction and data reported by others.

Table 1. Values of b/B from some references

Reference	Method of Analysis	Footing Type	Reinforcement Condition	Soil Type	b/B
Meyrhof [27]	Analytical	Strip	Unreinforced	Sand with $\phi=3^\circ 0-40^\circ$	5
Lee and Manjunath [28]	Experimental	Strip	Reinforced and Unreinforced	Sand with $\phi=38^\circ$	5
Choudhary et al. [10]	Experimental	Strip	Reinforced and Unreinforced	Flyash with $c=20$ kPa and $\phi=14^\circ$	3
El Sawwaf [7]	Experimental	Strip	Reinforced	Sand with $\phi=43^\circ$	2
Wing Ip [29]	Experimental	Strip	Unreinforced	Sand with $\phi=30^\circ$	6
Shin and Das [4]	Experimental	Strip	Reinforced	Clay	3
Castelli and Motta [30]	Analytical	Circular	Unreinforced	Undrained clay and sand with $\phi=0-40^\circ$	1-6
Present Study	Analytical	Strip	Reinforced and Unreinforced	Sand with $30^\circ-40^\circ$	3.1-5.4

b) Effect of reinforcement length on bearing capacity

The length of reinforcement layer has a significant effect on the footing bearing capacity. Figure 11 shows the results obtained from the developed analytical method. As seen, the reinforcement layer can vary between the slope face to the other side of the active wedge (see L_2 in Fig. 11). Therefore, if the

reinforcement length becomes greater than this distance, no improvement in the footing bearing capacity would be expected due to the fact that L_4 would not be effective (Fig. 11). Figure 11 shows that the total effective length is determined from:

$$L_{total} = L_2 + B + b + L_3 \tag{22}$$

$$H = B \tan(\eta_a) \tag{15 repeated}$$

$$L_1 = H / \tan(\eta_p) \tag{23}$$

$$L_1 = \frac{\tan \eta_A B}{\tan \eta_p} \tag{24}$$

Therefore:

$$L_2 = \frac{L_1}{H} (H - u) \tag{25}$$

From the slope geometry, the amount of L_3 is calculated as:

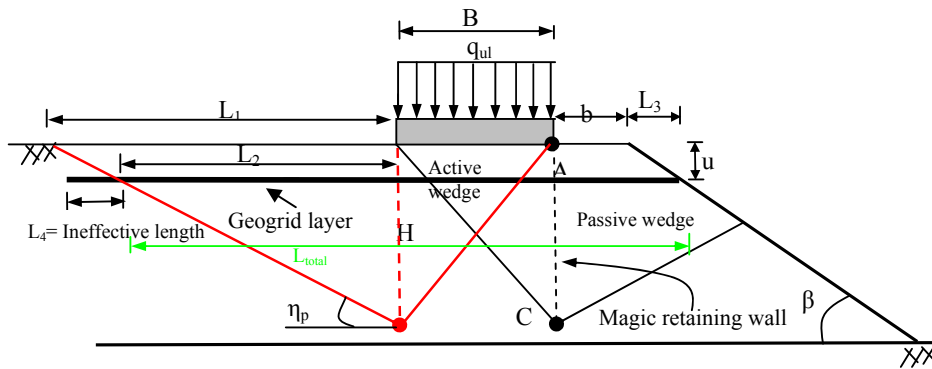


Fig. 11. Effective length of reinforcement layer

$$L_2 = \frac{1}{\tan \eta_p} [\tan \eta_A - n] B \tag{26}$$

$$L_3 = u / \tan \beta \tag{27}$$

Assuming $u = nB$, and $b = sB$:

$$L_{total} = \left[\frac{1}{\tan \eta_p} [\tan \eta_A - n] + (1 + s) + \frac{n}{\tan \beta} \right] B \tag{28}$$

Equation (28) indicates that the total effective length of the reinforcement layer depends on soil properties such as ϕ , foundation distance from slope crest, reinforcement location, and slope geometry. Figure 12 shows the effective reinforcement length versus ϕ for $s=1$, and $\beta=30^\circ$. As seen, for a given value of ϕ , for example 35° , the effective length decreases with increasing u . If u increases from $0.3B$ to $0.7B$, the reinforcement length decreases from $7B$ to $6.3B$. Figure 13 shows effective reinforcement length versus ϕ for $s=2$ and $\beta=25^\circ$. As observed, for $\phi=35^\circ$, the effective length decreases from $8.15B$ to $7.8B$ with increasing $u=0.3B$ up to $u=0.7B$. Yoo [5] stated that for optimum improvement in the ultimate bearing capacity of strip footing on a reinforced sandy slope, the length of reinforcement should be in the range of $5.5B-7B$.

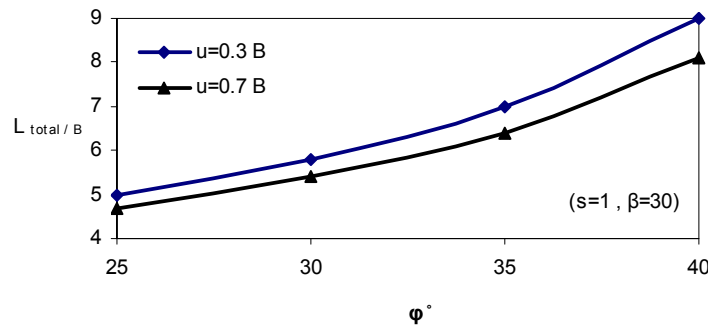


Fig. 12. Effective reinforcement length for s=1, β=30°

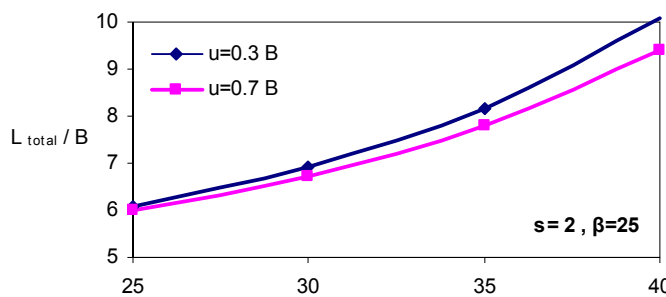


Fig. 13. Effective reinforcement length, s=2, β=25°

Lee and Manjunath [28] performed a series of numerical and small scale model tests to evaluate the bearing capacity of a strip footing on geogrid reinforced sand slope. They showed that the optimum reinforcement length was approximately equal to the edge distance plus 8B, which is measured from the face of the reinforced slope. Also, they performed numerical analysis and tests and obtained 8.9B. Based on the developed analytical study, for soil with φ=36°, slope angle of β=26.56°, and u=0.5 B for s=1, the total effective reinforcement layer becomes 7.49 B. The present analytical method gives effective lengths varying from 5.4B-8.1B for friction angles varying 30°-40° and for u = 0.7 B, β=30°, and s=1. These are in agreement with others as discussed.

c) Effect of soil relative density on reinforced bearing capacity

In this section, the BCR factor is used to identify the benefits of footing-soil reinforcement. Figure 14 indicates that the BCR value decreases with increasing the soil internal friction angle up to about 35°, beyond which no significant changes occur in the BCR values.

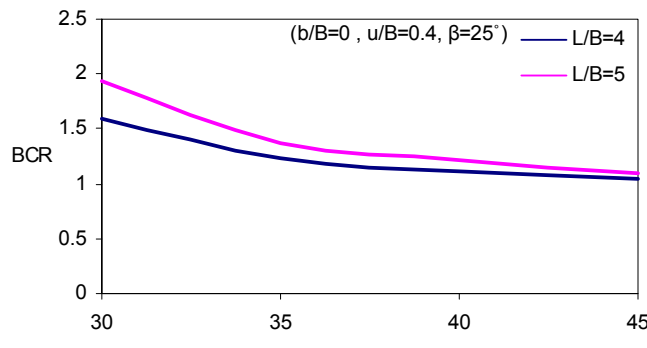


Fig. 14. Effect of reinforcement length on bearing capacity

d) Effect of number of reinforcement layers

In this section, some analyses are conducted to study the effect of N (number of reinforcement layer) on the bearing capacity of footings on the slope as presented in Fig. 15. Here, the reinforcement length and the distance of the footing from the slope edge were kept constant. As observed, with increasing N , the BCR increases, especially for lower soil friction angle.

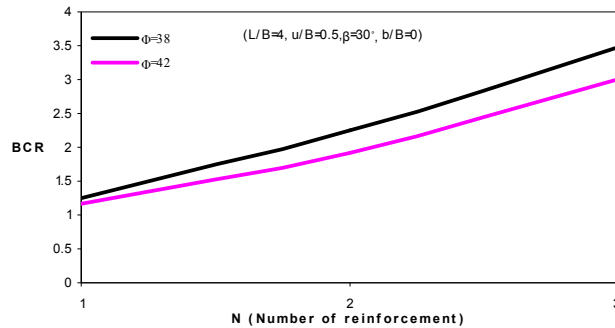


Fig. 15. Effect of variation of the number of reinforcement layer

The BCR value increases with increasing the number of geogrid layers located within the active and passive zones. Figure 3 shows that there is a limited zone depth for inclusion of reinforcement layers in order to have the footing bearing capacity improvement. This depth depends on soil properties, footing geometry, and slope geometry. As seen, the depth that reinforcement layers can be located varies within thickness H , i.e., between A to C points. This is in accordance with the findings of others. Alamshahi and Hataf [8] reported the increase in BCR only for two reinforcement layers beyond which the BCR value remained constant with increasing the number of reinforcement layers. Similar trends were reported by Lee and Manjunath [28]. El Sawwaf [7] performed two series of studies in order to investigate the effect of the number of geogrid layers on the footing-slope performance. The test series were carried out, a depth of replaced sand of $1.5B$ along with geogrid length, location, and spacing, was kept constant but the number of geogrid layers was varied. The results demonstrate that reinforcing a sand layer more than three layers of geogrid could bring about an improvement in bearing capacity greater than that obtained. El Sawwaf [7] performed tests on footing constructed on slopes which consisted of two layers. The upper layer was sand and the lower layer was clay. The sand thickness was $1.5B$. He reported that if u/B and b/B were constant, the footing bearing capacity did not have considerable increase when more than three geogrid layers were used. In the literature, there is no evidence that more than three geogrid layers have been used. This is because there exists a limited zone beneath the footing on the slope soil for reinforcement to achieve benefits on the BCR value. Figure 16 shows that for a certain slope geometry, limited reinforcement layers can be placed to have the footing bearing capacity improvement. Yoo [5], Lee and Manjunath [28] reported that there are a critical number of geogrid layers beyond which the BCR becomes constant. In this study, as depicted in Fig. 11, the reinforcement layers can only be located within AC zone to have BCR increase due to the soil reinforcement. This is because AC zone is equal to $H=B \tan \eta_A$. For a slope angle of 30° , if ϕ varies within a practical range of 30° - 45° for footing-soil reinforcement, H varies in $1.9B$ - $2.5B$ range. The above limitation was supported by Alamshahi and Hataf [8] in their tests. $h=0.75B$ was used for spacing of two reinforcement layers. They used only 2 geogrid layers within thickness AC in Fig. 11. Their results show that the third reinforcement layer did not have any effect on the footing bearing capacity. Based on analytical study present here, third reinforcement layer was located out of thickness AC, so it cannot affect the bearing capacity.

e) Effect of slope angle on BCR

Most research on the BCR of footings resting on reinforced soil slop used small scale tests with constant slope angles and the slope angle variation on the BCR variation has not been considered [27-5-7-8]. This paper considers this effect by using 10, 20, and 30° for the slope angles and the footing bearing capacity ratio versus these values are shown in Fig. 16. As seen, the BCR value increases with increasing the slope angle. It is interesting to note that the footing bearing capacity decreases obviously with increasing the slope angle. On the other hand, the use of reinforcement leads to increasing the bearing capacity of footings on slopes. In general, with increasing the slope angle, the latter grows more rapidly than the former, especially for steeper slopes. As a result, with increasing the slope angle, the footing bearing capacity ratio increases.

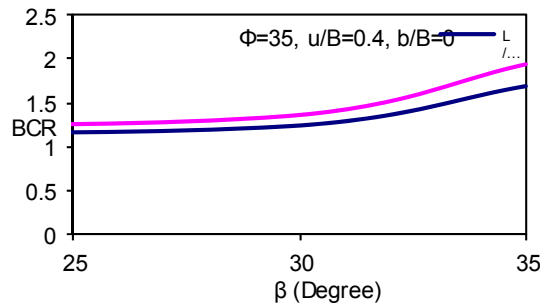


Fig. 16. Effect of slope angle on BCR

f) Determination of bearing capacity coefficient on reinforced sand slope

Equation (20) has been derived from the current analytical solution. This equation incorporates the effects of soil parameters, reinforcement material parameters, slope geometry, reinforcement layers, and reinforcement locations, and footing geometry. Figures 17 and 18 show the bearing capacity coefficients for reinforced soil slope for reinforcement lengths of 4B and 5B, respectively. As seen, the N_γ value increases with decreasing the slope angle.

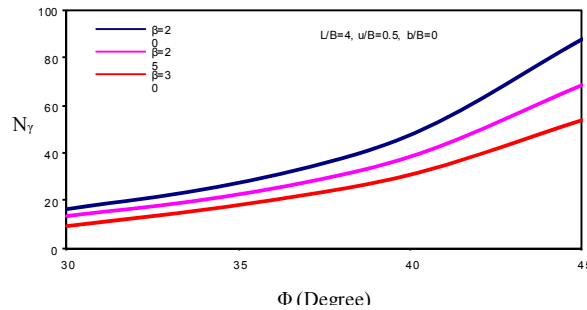


Fig. 17. Variation of N_γ versus ϕ for footing on reinforced sand slope (L/B=4)

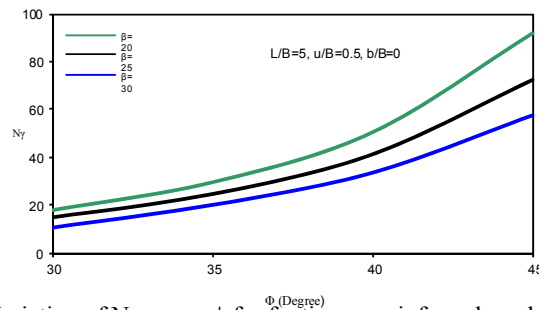


Fig. 18. Variation of N_γ versus ϕ for footing on reinforced sand slope (L/B=5)

6. CONCLUSION

In this paper, an analytical method for computing the ultimate bearing capacity of surface strip foundation on sandy slopes reinforced with geogrid layer are presented in which the Coulomb-type lateral earth pressure theory has been used. Based on the results predicted by this method, the following conclusions may be cited:

1. The magnitude of bearing capacity of strip footings on sandy slopes can be significantly increased by using geogrid layers.
2. The bearing capacity of footing decreases with increasing the slope angle for both unreinforced and reinforced sandy slopes. Also, the bearing capacity ratio increases with increasing the slope angle. This proves the reinforcement effect on the bearing capacity of footings on slopes.
3. The location of geogrid layers at a depth greater than 2.5 times the footing width does not have significant improvement on the bearing capacity. This study shows that the better depth for reinforcement location varies with soil properties, footing geometry and slope angle.
4. The slope geometry, reinforcement properties such as length, layer number, layer location, and soil properties has been found to have significant effects on the footing bearing capacity.

REFERENCES

1. Ghazavi, M. & Lavasan, A. A. (2008). Interference effect of shallow foundations constructed on sand reinforced with geosynthetics. *Geotextiles and Geomembranes*, Vol. 26, No. 5, pp. 404–415.
2. Khing, K. H., Das, B. M., Puri, V. K., Cook, E. E. & Yen, S. C. (1993). The bearing capacity of a strip foundation on geogrid reinforced sand. *Geotextiles and Geomembranes*, Vol. 12, pp. 351–361.
3. Omar, M., Das, B., Puri, V. & Yen, S. (1993). Ultimate bearing capacity of shallow foundations on sand with geogrid reinforcement. *Canadian Geotechnical Journal*, Vol. 30, pp. 545–549.
4. Shin, E. C., Das, B. M., Puri, V. K., Yen, S. C. & Cook, E. E. (1993). Bearing capacity of strip foundation on geogrid-reinforced clay. *Geotechnical Testing Journal, ASTM*, Vol. 16, No. 4, pp. 534–541.
5. Yoo, C. (2001). Laboratory investigation of bearing capacity behavior of strip footing on geogrid-reinforced sand slope. *Geotextiles and Geomembranes*, Vol. 19, pp. 279–298.
6. Vafaeian, M. & Abbaszadeh, R. (2006). Laboratory small scale tests to study the behaviour of reinforced soil wall. In: Kuwano, J., Kuseki, J. (Eds.), *Proceedings of Eighth International Conference on Geosynthetics*, Vol. 4. Millpress Science, Rotterdam, pp. 1409–1412.
7. El Sawwaf, M. (2007). Behaviour of strip footing on geogrid reinforced sand over a soft clay slope. *Geotextiles and Geomembranes*, Vol. 25, pp. 50–60.
8. Alamshahi, S. & Hataf, N. (2009). Bearing capacity of strip footings on sand slopes reinforced with geogrid and grid anchors. *Geotextiles and Geomembranes*, Vol. 27, pp. 217–226.
9. Sommers, A. N. & Viswanadham, B. V. S. (2009). Centrifuge model tests on behavior of strip footing on geotextile reinforced slopes. *Geotextiles and Geomembranes*, Vol. 27, pp. 497–505.
10. Choudhary, A. K., Jha, J. N. & Gill, K. S. (2010). Laboratory investigation of bearing capacity behaviour of strip footing on reinforced flyash slope, *Geotextiles and Geomembranes*, Vol. 28, pp. 393–402.
11. Michalowski, R. L. (2004). Limit loads on reinforced foundation soils. *Journal of Geotechnical and Geoenvironmental Engineering, ASCE*, Vol. 130, No. 4, pp. 381–390.
12. Huang, C. C. & Menq, F. Y. (1997). Deep-footing and wide slab effect in reinforced sandy ground. *Journal of Geotechnical and Geoenvironmental Engineering, ASCE*, Vol. 123, No. 1, pp. 30–36.
13. Sharma, R., Chen, Q. & Abu-Farsakh, M. (2008). Analytical modeling of geogrid reinforced soil foundation. *Geotextiles and Geomembranes*, Vol. 27, pp. 63–72.

14. Guido, V. A., Knueppel J. D. & Sweeny, M. A. (1987). Plate loading tests on geogrid reinforced earth slabs. *Proceedings Geosynthetics'87*, New Orleans, pp. 216-225.
 15. Huang, C., Tatsuoka, F. & Sato, Y. (1994). Failure mechanisms of reinforced sand slopes loaded with a footing. *Soils and Foundations*, Vol. 24, No. 2, pp. 27-40.
 16. Adams, Mike, T. & Collin, James, G. (1997). Large model spread footing load test on geosynthetic reinforced soil foundations. *Journal of Geotechnical Engineering, ASCE*, Vol. 123, No. 1, pp. 66-72.
 17. Patra, C. R., Das, B. M., Bhoi, M. & Shin, E. C. (2006). Eccentrically loaded strip foundation on geogrid-reinforced sand. *Geotextiles and Geomembranes*, Vol. 24, No. 4, pp. 254-259.
 18. Basudhar, P. K., Saha, S. & Deb, L. (2007). Circular footings resting on geotextile-reinforced sand bed. *Geotextiles and Geomembranes*, Vol. 25, No. 6, pp. 377-384.
 19. Sakti, J. & Das, B. M. (1987). Model tests for strip foundation on clay reinforced with geotextile layers. *Transportation Research Record No. 1153. National Academy of Sciences*, Washington, DC, pp. 40-45.
 20. Chen, H. T., Hung, W. Y., Chang, C. C., Chen, Y. J. & Lee, C. J. (2007). Centrifuge modeling test of a geotextile-reinforced wall with a very wet clayey backfill. *Geotextiles and Geomembranes*, Vol. 25, No. 6, pp. 346-359.
 21. Abu-Farsakh, M., Chen, Q., Sharma, R. & Zhang, X. (2010). Large-scale model footing tests on geogrid reinforced foundation and marginal embankment soils. *Geotechnical Testing Journal*, ASTM, (in press).
 22. Kumar, A. & Saran, S. (2003). Bearing capacity of rectangular footing on reinforced soil. *Geotechnical and Geological Engineering*, Vol. 21, pp. 201-224.
 23. Mosallanezhad, M., Hataf, N. & Ghahramani, A. (2010). Three dimensional bearing capacity analysis of granular soils reinforced with innovative grid-anchor system. *Iranian Journal of Science & Technology, Transaction B: Engineering*, Vol. 34, No. B4, pp. 419-431.
 24. Terzaghi, K. (1943). *Theoretical soil mechanics*. John Wiley and Sons, New York.
 25. Richards, R, Elms, D. G. & Budhu, M. (1993). Seismic bearing capacity and settlement of foundations. *Journal of Geotechnical Engineering*, Vol. 119, No. 4, pp. 662-74.
 26. Thanapalasingam, J. & Gnanendran, C. T. (2008). Predicting the performance of foundations near reinforced sloped fills. *12th International Conference of International Association for Computer Methods and Advances in Geotechnics*, Goa, India, pp. 3727-3734.
 27. Meyerhof, G. G. (1957). The ultimate bearing capacity of foundations on slopes. *Proceedings of the 4th International Conference on Soil Mechanics and Foundation Engineering*, Vol. 1, pp. 384-386.
 28. Lee, K. M. & Manjunath, V. R. (2000). Experimental and numerical studies of geosynthetic-reinforced sand slopes loaded with a footing. *Canadian Geotechnical Journal*, Vol. 37, pp. 828-842.
 29. Wing, Ip. (2005). Bearing capacity for foundation near slope. Mse. tesis, Concordia university, Montreal. Quebec, Canada
 30. Castelli, F. & Motta E. (2010). Bearing capacity of strip footings near slopes. *Geotechnical and Geological Engineering*, Vol. 28, No. 2, pp. 187-198.
-